Appl Phys B (2011) 105:749–760
DOI 10.1007/s00340-011-4711-0

Applied Physics B
Lasers and Optics

Optimization of Yb:YAG/Cr^{4+}:YAG composite ceramics passively Q-switched microchip lasers

J. Ma · J. Dong · K.-i. Ueda · A.A. Kaminskii

Received: 14 October 2010 / Revised version: 19 April 2011 / Published online: 12 October 2011
© Springer-Verlag 2011

Abstract The laser characteristics of laser-diode end-pumped Yb:YAG/Cr^{4+}:YAG composite ceramics microchip passively Q-switched lasers were studied by solving the coupled rate equations numerically taking into account the reabsorption of Yb:YAG ceramics at laser wavelength. Effects of the reflectivity of the output coupler, the concentrations and thickness of the saturable absorbers, and pump beam area on the laser performance were investigated analytically. The simulation results of the Yb:YAG/Cr^{4+}:YAG composite ceramics passively Q-switched microchip lasers were in good agreement with the experimental data. Better laser performance (high peak power, short pulse width and good optical-to-optical efficiency) of the composite Yb:YAG/Cr^{4+}:YAG ceramics passively Q-switched laser can be obtained by using a thin Cr^{4+}:YAG ceramic with high concentration, suitable reflectivity of the output coupler and proper pump beam diameter under high pump power intensity according to our simulations.

J. Ma · J. Dong (✉)
Department of Electronics Engineering, School of Information Science and Technology, Xiamen University, Xiamen 361005, P.R. China
e-mail: jdong@xmu.edu.cn

K.-i. Ueda
Institute for Laser Science, University of Electro-communications, 1-5-1 Chofugaoka, Chofu, Tokyo 182-8585, Japan

A.A. Kaminskii
Institute of Crystallography, Russian Academy of Sciences, Leninsky Prospekt 59, Moscow 119333, Russia

1 Introduction

Laser-diode pumped passively Q-switched microchip solid-state lasers are compact and simple single-mode lasers that emit sub-nanosecond pulses with high pulse energies and peak powers in a diffraction-limited output beam, and have many applications such as remote sensing, range finders, pollution detection, lidar, material processing, surgery, biological detection, laser ignition, and so on. The passively Q-switched microchip lasers are usually operated using a thin gain medium bonded with saturable absorber such as a semiconductor saturable-absorber mirror (SESAM) [1], bulk Cr^{4+}-ions doped crystals [2, 3], or depositing Cr^{4+}:YAG films on the gain medium by molecular beam epitaxy (MBE) [4]. Compared with SESAM or the Cr^{4+}:YAG film deposited on the surface of the gain medium, Cr^{4+}-ions doped bulk materials as saturable absorber have several advantages: high damage threshold, low cost, and simplicity. Compared with Nd:YAG laser materials, Yb:YAG laser materials have several advantages such as a long storage lifetime (951 μs) [5], a very low quantum defect (8.6% with pump wavelength of 941 nm and laser wavelength of 1030 nm), resulting in three times less heat generation during lasing than comparable Nd-based laser systems [6], broad absorption bandwidth and less sensitive to diode wavelength specifications [7], a smaller emission cross section [8] suitable for Q-switching operation, and easy growth of high quality crystals without concentration quenching [9]. Self-Q-switched laser crystals have been successfully grown by co-doping Cr^{4+} ions and Yb^{3+} ions or Nd^{3+} ions in garnet laser crystal hosts [10, 11]. Compact laser-diode pumped Cr,Yb:YAG self-Q-switched microchip laser with pulse width of 440 ps and peak power of over 53 kW has been demonstrated [12]. However, owing to co-doping of chromium ions with Yb into YAG host, the fluorescence

lifetime decreases [13] with increase of Cr concentration and there is strong absorption (about 60% of that around 1 μm) of pump power by Cr^{4+}-ions at pump wavelength (around 940 nm) owing to the broad absorption spectrum of Cr^{4+}:YAG from 800 nm to 1300 nm [14, 15]. High pump power threshold is caused by the high intracavity loss induced by the defects introducing Cr and Ca ions into Yb:YAG crystal to form Cr,Yb:YAG self-Q-switched laser crystal. Passively Q-switched microchip lasers by sandwiching Cr^{4+}:YAG saturable absorber between gain medium and output coupler, proposed by J.J. Zayhowski about two decades ago [16] is an alternative way to overcome pump power absorption loss from Cr^{4+}:YAG and to achieve highly efficient laser operation with short pulse width in passively Q-switched Yb:YAG/Cr^{4+}:YAG microchip lasers. Short resonator cavity length permits short pulse generation. Separation of gain medium and saturable absorber eliminates the defects introducing in Cr,Yb:YAG crystal. Passively Q-switched Yb:YAG/Cr^{4+}:YAG microchip lasers with sub-nanosecond pulse width have been demonstrated [17]. However, there is loss and air gap between the interface of Cr^{4+}:YAG and Yb:YAG, the laser operation is less efficient, and potential energy storage of Yb:YAG crystal cannot be fully extracted. The air gap also significantly affects the Q-switched laser performance by etalon effect in the resonator [18] and limits the scaling of peak power because of potential air breakdown at high intracavity intensity.

Transparent laser ceramics fabricated by modern ceramic sintering technology have attracted lots of attentions in solid-state laser fields. Efficient, high power lasers based on ytterbium or neodymium ions doped isotropic laser ceramics have been achieved in the last decade [19–21]. Efficient continuous-wave Yb:YAG ceramic lasers [21, 22] and passively Q-switched Yb:YAG/Cr^{4+}:YAG all-ceramics microchip lasers have been demonstrated [23, 24]. Most impressive research works based on the sintering ceramic technology [25] is to fabricate multifunctional composite materials for compact optics system applications [26]. Yb:YAG/Cr^{4+}:YAG composite ceramics provide an effective way to build compact passively Q-switched microchip lasers with efficient, sub-nanosecond, and high peak power pulsed laser output. Composite ceramics not only decrease the intracavity loss between the interface of Yb:YAG and Cr^{4+}:YAG, but also eliminate the air gap between these two parts to avoid the air breakdown under high intracavity intensity. Optical properties of Yb:YAG/Cr^{4+}:YAG composite ceramics and laser performance of Yb:YAG/Cr^{4+}:YAG composite ceramics passively Q-switched laser by using plane-concave cavity have been reported [26]. Highly efficient, sub-nanosecond pulse width and high peak power laser operation has been achieved in Yb:YAG/Cr^{4+}:YAG composite ceramics [26, 27]. Laser pulses with pulse energy of 172 μJ, pulse width of 237 ps, and peak power of over 0.72 MW have been achieved with Yb:YAG/Cr^{4+}:YAG composite ceramics, these are, to our knowledge, the shortest Q-switched pulse width ever achieved in passively Q-switched Yb:YAG/Cr^{4+}:YAG microchip lasers.

Although Yb:YAG/Cr^{4+}:YAG composite ceramics can be fabricated easier than traditional optical bonding of Yb:YAG/Cr^{4+}:YAG crystals, the doping concentrations of ytterbium ions and chromium ions in Yb:YAG and Cr^{4+}:YAG parts have to be fully considered before a practical laser system is built. The performance and optimization of laser-diode pumped passively Q-switched lasers is usually analyzed by solving coupled rate equations. Motivated by their research work on passively Q-switched microchip lasers, Zayhowski and Kelly analyzed the rate equations for rapid Q-switching [28]. Simple expressions for the maximum peak power, maximum pulse energy, and minimum pulse width were derived for different output couplings under fixed pump power. There are also lots of theoretical investigations on passively Q-switched solid-state lasers with Cr^{4+}:YAG as saturable absorber by adopting coupled rate equations, most of them are focused on Nd^{3+}-ions doped solid-state materials [29–32]. Because the optical properties of Yb:YAG is different from those of Nd-ions doped solid-state materials, especially the quasi-three-level nature of Yb:YAG material and the reabsorption of Yb:YAG at laser wavelength of 1030 nm is totally different form the four-level system of Nd lasers. Therefore, some theoretical works on passively Q-switched Yb:YAG lasers with Cr^{4+}:YAG as saturable absorber have been proposed and the numerical simulations are in good agreement with experimental data [33, 34]. However, there are no references which investigate the effects of concentration and thickness of saturable absorber on the laser performance (pulse energy, pulse width, peak power and repetition rate) at fixed pump power intensity. Although good agreements and predictions of laser performance can be achieved by numerically solving the coupled rate equations, it is tedious and time-costly. Therefore, a simple analytical method is needed to predict the performance of passively Q-switched lasers.

In this paper, motivated by our research work on highly efficient, high peak power, sub-nanosecond Yb:YAG/Cr^{4+}:YAG composite ceramics passively Q-switched lasers, we present the numerical simulations of a laser-diode pumped Yb:YAG/Cr^{4+}:YAG composite ceramics passively Q-switched laser. The modified coupled rate equations of passively Q-switched laser taking accounting into the reabsorption of Yb:YAG ceramics were given and the numerical solutions of the rate equations agreed well with the experimental results [27]. The simple analytical method was used to solve the transcendental equation connecting final inversion population with initial inversion population and threshold inversion population for passively Q-switched lasers. The effects of the reflectivity of the

output coupler, concentration and thickness of Cr^{4+}:YAG ceramic, and pump beam waist on the performance of the Yb:YAG/Cr^{4+}:YAG composite ceramics passively Q-switched lasers were investigated analytically. Practical design guidelines for Yb:YAG/Cr^{4+}:YAG composite ceramics passively Q-switched microchip lasers were given for achieving high peak power while maintaining high efficiency.

2 Model of passively Q-switched microchip laser

According to the passively Q-switched laser theory [29, 32, 35, 36], the modified coupled rate equations of photon density, population inversion density of gain medium and the saturable absorber in the passively Q-switched resonator, which include the excited-state absorption of the saturable absorber, the pump term, and the reabsorption loss of quasi-three-level laser medium, are given by

$$\frac{d\phi}{dt} = \frac{\phi}{t_r}\left(2\sigma Nl - 2\sigma_g N_g l_s - 2\sigma_e N_e l_s - \ln\left(\frac{1}{R}\right) - L - 2\alpha_L l\right) \tag{1}$$

$$\frac{dN}{dt} = -\gamma\sigma c\phi N - \frac{N}{\tau} + W_p \tag{2}$$

$$\frac{dN_g}{dt} = -\sigma_g c\phi N_g + \frac{N_{s0} - N_g}{\tau_s} \tag{3}$$

$$N_g + N_e = N_{s0} \tag{4}$$

where ϕ is the photon density in the laser cavity of optical length l_c, N is the population inversion density of the gain medium, σ is the stimulated emission cross section of the laser medium, t_r is the cavity round-trip time, $t_r = 2l_c/c$, l is the length of the laser gain medium, c is the speed of the light in vacuum, σ_g and σ_e are the absorption cross sections of ground state and excited state of the saturable absorber, l_s is the length of the saturable absorber, N_g and N_e are the ground state and excited-state population density of the saturable absorber, respectively, N_{s0} is the total population density of the saturable absorber; α_L is the absorption coefficient at lasing wavelength of gain medium, R is the reflectivity of the output coupler, L is the nonsaturable intracavity round-trip dissipative optical loss, γ is the inversion reduction factor, $\gamma = 2$ for Yb^{3+} doped three-level solid-state lasers, W_p is the volumetric pump rate into the upper laser level and is proportional to the continuous-wave pump power, $W_p = P_p[1 - \exp(-\alpha l)]/(h\nu_p A_p l)$, P_p is the incident pump power, $h\nu_p$ is the pump photon energy, A_p is the pump beam area, α is the absorption coefficient of gain medium at pump wavelength, τ is the lifetime of the upper laser level of the gain medium, and τ_s is the excited-state lifetime of the saturable absorber.

Because the buildup time of the Q-switched laser pulse is generally quite short compared with the pumping and relaxation time of the gain medium, it is reasonable to neglect the effect of pumping and spontaneous decay of the laser population inversion density during pulse generation; with this assumption, (2) becomes,

$$\frac{dN}{dt} \cong -\gamma c\sigma\phi N \tag{5}$$

When the photon intensity is low, almost all the population of the saturable absorber is in the ground state, hence we can approximate the initial population inversion density before saturation of the saturable absorber by setting the right-hand side of (1) to zero and assume that $N_g = N_{s0}$, so the initial population inversion density can be written as,

$$N_i = \frac{2\sigma_g N_{s0} l_s + \ln(\frac{1}{R}) + L + 2\alpha_L l}{2\sigma l} \tag{6}$$

When the photon intensity is high, most of the population in the ground state of the saturable absorber is excited to the excited state. Therefore, we can approximate the population inversion density after the bleaching of the saturable absorber by setting the right-hand side of (1) to zero and assuming that $N_g \cong 0$, and the threshold population inversion density can be written as,

$$N_{th} \cong \frac{2\sigma_e N_{s0} l_s + \ln(\frac{1}{R}) + L + 2\alpha_L l}{2\sigma l} \tag{7}$$

With expression (7) we can rewrite (1) as

$$\frac{d\phi}{dt} = \frac{\phi}{t_r}(2\sigma Nl - 2\sigma N_{th} l) \tag{8}$$

Dividing expression (8) by expression (5) gives,

$$\frac{d\phi}{dN} = -\frac{l}{l_c}\frac{N - N_{th}}{\gamma N} \tag{9}$$

Equation (9) can be integrated from the time of Q-switch opening to an arbitrary time t by

$$\int_{\phi_i}^{\phi(t)} d\phi = -\frac{l}{l_c\gamma}\int_{N_i}^{N(t)}\left(1 - \frac{N_{th}}{N}\right)dN \tag{10}$$

Initial photon density ϕ_i is small compared with the value of ϕ anytime during the laser output pulse. Hence the solution of expression (10) is

$$\phi(t) \cong \frac{l}{l_c\gamma}\left[N_i - N - N_{th}\ln\left(\frac{N_i}{N}\right)\right] \tag{11}$$

As can be inferred from expression (8), the photon number reaches a peak value ϕ_{peak} when N is equivalent to N_{th}.

Hence from expression (11), we have

$$\phi_{\text{peak}} \cong \frac{l}{l_c\gamma}\left[N_i - N_{\text{th}} - N_{\text{th}}\ln\left(\frac{N_i}{N_{\text{th}}}\right)\right] = \frac{lN_i}{l_c\gamma}\left[\frac{N_i/N_{\text{th}} - 1 - \ln(N_i/N_{\text{th}})}{N_i/N_{\text{th}}}\right] \tag{12}$$

Expression (12) indicates that, when N_i/N_{th} approaches infinity, the peak photon number approaches the maximum available population inversion density $lN_i/l_c\gamma$.

After the release of the Q-switched laser pulse, laser population inversion density N is depleted by the photon flux and is reduced to a value below N_{th}. We can derive this final population inversion density N_f from expression (11) by setting $\phi \cong 0$ because the photon density is small after the release of the Q-switched laser pulse. Let $N = N_f$ and $\phi = 0$; then expression (11) becomes

$$N_i - N_f - N_{\text{th}}\ln\left(\frac{N_i}{N_f}\right) = 0 \tag{13}$$

Expression (13) is transcendental and can be solved numerically. When N_i and N_f are known, the output pulse energy E, peak power P and pulse width τ_p of Yb:YAG/Cr^{4+}:YAG composite ceramics passively Q-switched microchip laser can be written as [29]

$$E = \frac{h\nu A}{2\sigma\gamma}\ln\left(\frac{1}{R}\right)\ln\left(\frac{N_i}{N_f}\right) \tag{14}$$

$$P = \frac{h\nu Al}{\gamma t_r}\ln\left(\frac{1}{R}\right)\left[N_i - N_{\text{th}} - N_{\text{th}}\ln\left(\frac{N_i}{N_{\text{th}}}\right)\right] \tag{15}$$

$$\tau_p \approx \frac{E}{P} \tag{16}$$

where $h\nu$ is the photon energy, and A is the active area of the beam in the laser medium.

Expression (11)–(16) may be used to quantitatively evaluate the performance of a laser that is passively Q-switched with a slow-relaxing saturable absorber without actually executing the numerical calculation. N_i, N_{th}, N_f are the population inversion densities at the start of Q-switching, the point of maximum peak power and the end of the Q-switched pulse, respectively.

With continuous-wave pumping, the laser will be passively Q-switched as soon as the gain exceeds the combined saturable and unsaturable losses in the resonator. As the incident pump power is increased, the laser eventually reaches a threshold condition and starts to repetitively Q-switched operation with a time interval between pulses, t_c. For continuous-wave pumped repetitive Q-switching laser at a repetition rate f, the maximum time available for the inversion to build up between pulses is $t_c = 1/f$. Therefore,

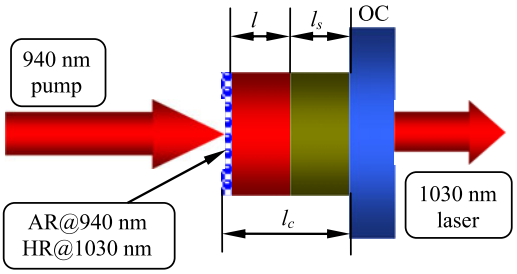

Fig. 1 The experimental setup of laser-diode pumped Yb:YAG/Cr^{4+}:YAG composite ceramics passively Q-switched laser. OC is the output coupler

the initial inversion density of the Q-switch under the influence of the absorbed pump power can be written as [32]

$$N_i = N_{\text{cw}} - (N_{\text{cw}} - N_f)\exp\left(\frac{-1}{\tau f}\right) \tag{17}$$

in order to have the population inversion return to its original value after each Q-switch cycle, where N_{cw} is the continuous-wave pumping inversion population density inside the resonator. Equations (17) and (13) can be solved numerically to obtain the initial inversion density, N_i and final inversion density, N_f for continuous-wave pumped repetitively Q-switched lasers.

3 Configuration of passively Q-switched microchip laser

The schematic diagram of a laser-diode end-pumped Yb:YAG/Cr^{4+}:YAG composite ceramics passively Q-switched laser is shown in Fig. 1. A monolithic coated Yb:YAG/Cr^{4+}:YAG composite ceramics was used to form a resonator. The Yb^{3+}-ions doping concentration of Yb:YAG ceramic is C_{Yb}, and the Cr ions doping concentration of Cr^{4+}:YAG ceramic is C_s. The thickness of Yb:YAG ceramic is l, and the thickness of Cr^{4+}:YAG ceramic is l_s, varying from 0.1 mm to 3.4 mm depending on the doping concentration of Cr ions. Therefore the total thickness of the monolithic Yb:YAG/Cr^{4+}:YAG composite ceramics is $l + l_s$. The Yb:YAG ceramic surface facing the pump beam was coated for high reflectivity at 1030 nm and antireflection at pump wavelength of 940 nm. The other surface of the composite ceramic was coated with antireflection at 1030 nm to reduce the intracavity loss. An plane-parallel output coupler with reflectivity of R at 1030 nm was attached tightly to the Yb:YAG/Cr^{4+}:YAG composite ceramics. Therefore, the total cavity length, l_c, is $l + l_s$. A commercial available fiber-coupled laser-diode working at central wavelength of 940 nm was used as pump source, the numerical aperture is 0.22. The Rayleigh length of the pump beam after optical coupling system is within the range of one centimeter depending on the focus spots required in the laser system.

Table 1 The parameters used for modeling of Yb:YAG/Cr^{4+}:YAG composite ceramics passively Q-switched lasers

	Constant	Value	Ref.
Emission cross section of Yb:YAG ceramic	σ	2.2×10^{-20} cm^2	[21, 40]
Absorption cross section of Cr^{4+}:YAG	σ_g	4.6×10^{-18} cm^2	[41–43]
Excited-state absorption cross section of Cr^{4+}:YAG	σ_e	8.2×10^{-19} cm^2	[43]
Lifetime of Yb:YAG ceramic	τ	951 μs	[5, 40]
Lifetime of Cr^{4+}:YAG ceramic	τ_s	3.4 μs	[43]
Pump photon energy	$h\nu_p$	2.12×10^{-19} J	
Laser photon energy	$h\nu$	1.93×10^{-19} J	
Loss	L	0.05	
Yb^{3+} ions concentration	C_{Yb}	10 at%	
Cr^{4+} ions concentration	N_{s0}	5×10^{17} cm^{-3}	
Thickness of Yb:YAG ceramic	l	1.2 mm	
Thickness of Cr^{4+}:YAG ceramic	l_s	1.5 mm	
Pump wavelength	λ_p	940 nm	
Laser wavelength	λ	1030 nm	
Pump beam waist	w_p	66 μm	
Laser beam waist	w_L	60 μm	

4 Numerical simulations

The numerical simulations of laser pulse trains and pulse profiles of Yb:YAG/Cr^{4+}:YAG composite ceramics passively Q-switched lasers were done by numerically solving (1)–(4) with Runge–Kutta method based on the parameters obtained in the laser experiments [27]. Because 2.7-mm-thick Yb:YAG/Cr^{4+}:YAG composite ceramics [27] is less than the Rayleigh length of the pump beam used in the experiments, the effective laser beam area on the laser gain medium can be assumed to be equal to that on the saturable absorber for the Yb:YAG/Cr^{4+}:YAG composite ceramics passively Q-switched microchip laser. And it is reasonable to assume that the pump beam diameter inside the Yb:YAG/Cr^{4+}:YAG composite ceramics does not change along the pump axis. The parameters used in the numerical simulations are taken from the experimental condition of Yb:YAG/Cr^{4+}:YAG composite ceramics passively Q-switched lasers [27] and listed in Table 1.

Figure 2(a) shows the numerical stimulation of the pulse train of the Yb:YAG/Cr^{4+}:YAG composite ceramics passively Q-switched lasers under incident pump power of 4.5 W. It takes about 235 μs to develop the first Q-switched laser pulse, the time interval between subsequent Q-switched laser pulses is about 170 μs, which is shorter than that required for developing the first laser pulse because inversion density, N, does not decrease to zero after the release of the first laser pulse. The repetition rate is estimated to be 5.7 kHz, which is higher than that of 4 kHz measured in experiments under the same pump power level [27]. Figure 2(b) is an expanded picture of Fig. 2(a) near the occurrence of the first laser pulse. When the photon density inside the laser cavity increases, the loss decreases accordingly as a result of the bleaching effect of the Cr^{4+}:YAG saturable absorber. The photon density reaches its peak value when the gain equals the cavity loss, i.e., when $N = N_{\mathrm{th}} = 1.56 \times 10^{20}$ cm^{-3}, corresponding to the value calculated by (7). Beyond this point the laser inversion density (gain) is smaller than the total loss of the laser system, and the Q-switched laser pulse dies out quickly while the laser inversion population decreases gradually to a minimum value of $\sim 8.78 \times 10^{19}$ cm^{-3}. The increase of the loss after the release of the Q-switched laser pulse is due to the relaxation of the saturable absorber population. The initial laser inversion population required for laser action, 2.54×10^{20} cm^{-3}, calculated by (6), is lower than that obtained by numerical simulation, 2.55×10^{20} cm^{-3}. The cause of this difference is that we assume that $N = Loss/2\sigma l$ in deriving (6), whereas it is required that $N > Loss/2\sigma l$ for the laser action to occur. The pulse width (full width at half-maximum) is about 200 ps, as shown in Fig. 2(b). The output pulse energy is about 180 μJ, which is calculated by integration of the Q-switched laser pulse over a time range covering the entire laser pulse according to the expression [32]

$$E_{\mathrm{out}} = \frac{h\nu_l A l \ln(1/R)}{2l_c/c} \int_0^\infty \phi(t)\, dt \tag{18}$$

so the peak power was determined to be 900 kW. The average output power of 1 W was obtained at incident pump power of 4.5 W, corresponding to optical-to-optical efficiency of 22% with respect to the incident pump power.

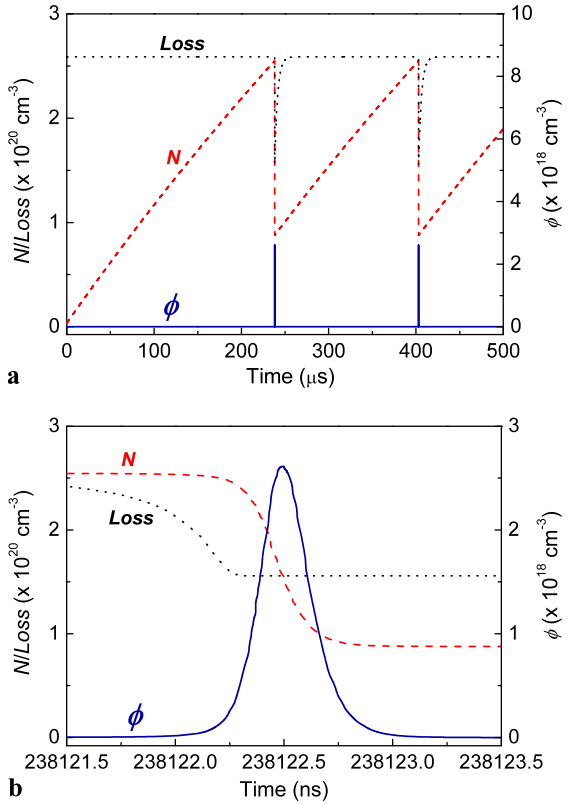

Fig. 2 The numerical calculations of laser pulse train and the dynamic of the pulse development for laser-diode pumped Yb:YAG/Cr^{4+}:YAG composite ceramics passively Q-switched laser. (**a**) Evolution of the photon density, gain inversion density and the loss on the time scale of the repetition period for pump power of 4.5 W; (**b**) evolution of the photon density, gain inversion density and the loss on the time scale of the pulse width

The calculated pulse energy of 180 μJ and pulse width of 200 ps are in fair agreement with the experimentally obtained pulse energy of 172 μJ and pulse width of 237 ps [27]. The remaining discrepancies between the numerically calculated results and the experimental data may be caused by the precise concentration of the Cr^{4+} ions in the Cr^{4+}:YAG ceramic, the pump beam variation along the thickness of Yb:YAG/Cr^{4+}:YAG ceramics, and the beam diameter of the laser output. Furthermore, the thermal lens is one critical factor for forming stable laser cavity in a plane-parallel resonator, and it is not taken into account in the numerical simulation.

5 Analytical simulations and prediction

Although good agreements and predictions of laser performance can be achieved by numerically solving the rate equations, it is tedious to repetitively calculate the coupled rate equations to predict the laser performance of passively Q-switched microchip lasers. Therefore, following simple analytical method was proposed to predict the performance of passively Q-switched lasers. From (14) and (15), we can see that the pulse energy and peak power are governed by the laser beam area, A, reflectivity of output coupler, R, initial inversion population, N_i, the threshold population inversion density, N_{th}, and final inversion population, N_f. Initial inversion population, N_i, and threshold inversion population density, N_{th}, are determined by (6) and (7), respectively. Final inversion population, N_f, is related to N_i and N_{th} through transcendental equation (13). N_i, N_{th}, and N_f are all relative to the initial transmission of saturable absorber, T_0, and reflectivity of output coupler, R. Therefore, the pulse energy, peak power and pulse width are all determined by the laser beam area, A, reflectivity of output coupler, R, and initial transmission of saturable absorber, T_0. The transcendental equation (13) can be solved analytically with the aid of Lambert W-function [37]. Lambert W-function has the property of $x = W(x)\exp[W(x)]$ [38]. Transcendental equation (13) was changed in form as $N_i - N_f = N_{\text{th}} \ln(N_i/N_{\text{th}})$. Then, we took the exponential on both sides of the equation and changed the form into

$$-N_{\text{th}}\left(-\frac{N_f}{N_{\text{th}}}\right)\exp\left(-\frac{N_f}{N_{\text{th}}}\right) = N_i \exp\left(-\frac{N_i}{N_{\text{th}}}\right) \tag{19}$$

Let $W(x) = -N_f/N_{\text{th}}$; then (19) becomes

$$-N_{\text{th}} W(x)\exp\big[W(x)\big] = N_i \exp\left(-\frac{N_i}{N_{\text{th}}}\right) \tag{20}$$

Comparing (20) with $x = W(x)\exp[W(x)]$, then, $x = -\frac{N_i}{N_{\text{th}}}\exp(-\frac{N_i}{N_{\text{th}}})$. With expression $W(x) = -N_f/N_{\text{th}}$, N_f was obtained as follows,

$$N_f = -N_{\text{th}} W\left[-\frac{N_i}{N_{\text{th}}}\exp\left(-\frac{N_i}{N_{\text{th}}}\right)\right] \tag{21}$$

Therefore, effects of doping concentration and thickness of saturable absorber, reflectivity of output coupler and pump beam diameter on the laser performance of Yb:YAG/Cr^{4+}:YAG passively Q-switched microchip lasers can be fully analyzed.

Firstly, the effect of reflectivity of output coupler on the Yb:YAG/Cr^{4+}:YAG composite ceramics passively Q-switched lasers was investigated analytically by solving (21). The incident pump power of 4.5 W was used in the simulations. And the other optical parameters of Yb:YAG/Cr^{4+}:YAG composite ceramics used in simulations were listed in Table 1. The corresponding pump power intensity is about 33 kW/cm^2, which is higher enough to obtain efficient laser oscillation at room temperature for Yb:YAG gain medium [39]. Figure 3 shows the calculated pulse energy, the pulse width, the peak power, the repetition rate, and the average output power of Yb:YAG/Cr^{4+}:YAG composite ceramics passively Q-switched laser as a function of R for different Cr^{4+} concentrations. When the thickness of Cr^{4+}:YAG ceramic is fixed to 1.5 mm, the pulse energy decreases with

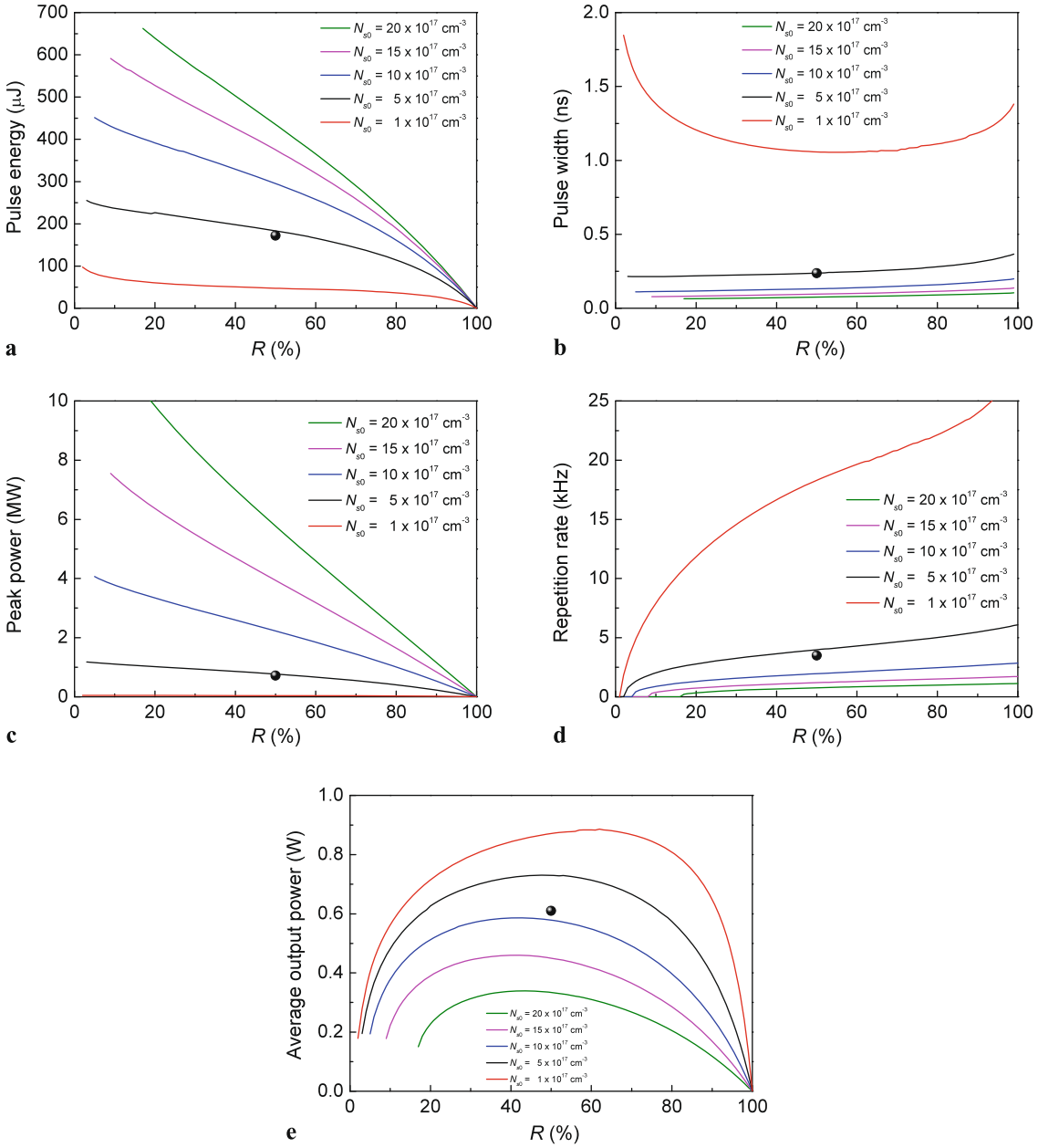

Fig. 3 (**a**) Pulse energy, (**b**) pulse width, (**c**) peak power, (**d**) repetition rate and (**e**) average output power as a function of the reflectivity of output coupler for different concentrations of Cr^{4+}:YAG ceramic under incident pump power of 4.5 W. The solid dots are the experimental data under incident pump power of 4.5 W taken from Ref. [27]

R for different concentrations of Cr^{4+}:YAG ceramics, the larger the reflectivity of the output coupler, the lower the pulse energy. The pulse energy increases with concentrations of Cr^{4+}:YAG ceramic, the higher the concentrations of Cr^{4+}:YAG ceramic, the higher the pulse energy, as shown in Fig. 3(a). The effect of Cr^{4+} concentration on the pulse energy becomes smaller at high Cr^{4+} concentration levels (e.g. $N_{s0} > 10 \times 10^{17}$ cm^{-3}). The pulse width increases with R when Cr^{4+} concentration is higher than 5×10^{17} cm^{-3}. There is an optimum reflectivity of the output coupler (about 62%) to obtain minimum pulse width when Cr^{4+} concentration is 1×10^{17} cm^{-3}, as shown in Fig. 3(b). Pulse width decreases with Cr^{4+} concentration and becomes no sensitive to the Cr^{4+} concentration at high Cr^{4+} concentration. The peak power decreases with R for different concentrations of Cr^{4+}:YAG ceramic. When the reflectivity of output coupler is fixed, the peak power increases with concentrations of Cr^{4+}:YAG ceramic, the higher the concentration of Cr^{4+}:YAG ceramic, the higher the peak power, as shown in Fig. 3(c). The repetition rate increases with R for different

concentrations of Cr^{4+}:YAG ceramic. When the reflectivity of output coupler is fixed, the repetition rate decreases with concentrations of Cr^{4+}:YAG ceramic and is very sensitive to the concentration of Cr^{4+}:YAG ceramic when the concentrations of Cr^{4+}:YAG ceramic is low, the lower the concentrations of Cr^{4+}:YAG ceramic, the higher the repetition rate, as shown in Fig. 3(d). The average output power decreases with concentrations of Cr^{4+}:YAG ceramic, there is a optimum reflectivity of the output coupler to achieve the maximum average output power for different concentrations of Cr^{4+}:YAG ceramic, as shown in Fig. 3(e). The optimum reflectivity of the output couplers are 62, 48, 42, 42 and 42% for $N_{s0} = 1 \times 10^{17}$, 5×10^{17}, 10×10^{17}, 15×10^{17}, 20×10^{17}, cm^{-3}, respectively. The optimum reflectivity of the output coupler becomes smaller with concentration of Cr^{4+}:YAG ceramic. The optimum reflectivity of the output coupler nearly keeps constant when the concentration of Cr^{4+}:YAG ceramic is higher than 5×10^{17} cm^{-3}. From Fig. 3, we can see that there is an optimum reflectivity of the output coupler to obtain the maximum average output power, therefore, the reflectivity of the output coupler should be chosen based on the highest optical-to-optical efficiency, e.g. the highest average output power achievable under certain doping concentration of Cr^{4+}:YAG ceramic. The simulated results show that a better Yb:YAG/Cr^{4+}:YAG passively Q-switched laser, such as short pulse width, high pulse energy output and high average output power, can be obtained by choosing a Cr^{4+}:YAG ceramic saturable absorber with high Cr^{4+} concentration and with suitable reflectivity of output coupler (around 50%).

From Fig. 3, for Cr^{4+} concentration of 5×10^{17} cm^{-3}, laser pulse with over 184 μJ pulse energy, pulse width of 238 ps at repetition rate of 4 kHz was obtained when R is set to 50%, which was corresponding to the experimental conditions of Yb:YAG/Cr^{4+}:YAG composite ceramics passively Q-switched lasers. The corresponding peak power of over 0.77 MW was achieved. The average output power of 730 mW was obtained at incident pump power 4.5 W, the corresponding optical-to-optical efficiency of 23% with respect to the absorbed pump power can be obtained. These calculated results are in good agreement with the experimental pulse energy of 172 μJ, pulse width of 237 ps, and peak power of 0.72 MW [27]. The calculated laser characteristics of Yb:YAG/Cr^{4+}:YAG composite ceramics passively Q-switched microchip lasers with Lambert W-function are more accurate comparing to the simulation results by numerically solving coupled rate equations. Therefore, solving transcendental equation analytically with the aid of Lambert W-function is a more effective and simple way to analyze the laser performance of passively Q-switched solid-state lasers.

Secondly, the effect of the thickness of Cr^{4+}:YAG ceramic on the laser performance of Yb:YAG/Cr^{4+}:YAG composite ceramics passively Q-switched laser was investigated analytically. When the concentration of Cr^{4+}:YAG ceramics is fixed, the thickness of the Cr^{4+}:YAG ceramic governs the initial transmission of saturable absorber, and the initial transmission of saturable absorber decreases with the thickness of Cr^{4+}:YAG ceramic. Figure 4 shows the pulse energy, pulse width, peak power, repetition rate and average output power as a function of the thickness of Cr^{4+}:YAG ceramic for different concentrations of Cr^{4+}:YAG ceramics when the reflectivity of output coupler was set to 50%. The incident pump power of 4.5 W and pump beam diameter of 132 μm were used in the calculation, and the corresponding pump power intensity is about 33 kW/cm^2.

From Fig. 4(a), the pulse energy increases with thickness of Cr^{4+}:YAG ceramic for different Cr^{4+} concentrations, the higher the Cr^{4+} concentration, the higher the output pulse energy. For Cr^{4+}:YAG with high Cr^{4+} concentration, the pulse energy is limited by inversion population provided by the pump power used in the simulation (4.5 W) to overcome the laser oscillation threshold owing to the low initial transmission of thick Cr^{4+}:YAG. As indicated in Fig. 4(b), the pulse width is very sensitive to the length of Cr^{4+}:YAG ceramic and varies from several ns to 0.5 ns rapidly with thickness of Cr^{4+}:YAG ceramic when the thickness of Cr^{4+}:YAG ceramic is shorter than 0.5 mm. The pulse width decreases slowly with the thickness of Cr^{4+}:YAG ceramic when the thickness of Cr^{4+}:YAG ceramic is larger than 0.5 mm for different Cr^{4+} concentrations. The peak power increases with the thickness of Cr^{4+}:YAG ceramic for different Cr^{4+} concentrations, the higher the Cr^{4+} concentration, the higher the peak power, as shown in Fig. 4(c). The repetition rate decreases dramatically with the thickness of Cr^{4+}:YAG ceramic when the thickness of Cr^{4+}:YAG ceramic is less than 0.5 mm and then decreases slowly with thickness of Cr^{4+}:YAG ceramic for different Cr^{4+} concentrations, the higher the Cr^{4+} concentration, the lower the repetition rate, as shown in Fig. 4(d). The average output power decreases with the thickness of Cr^{4+}:YAG ceramic for different Cr^{4+} concentrations, and this effect becomes remarkable for high Cr^{4+} concentrations, as shown Fig. 4(e). From Fig. 4, we can also see that the same pulse energy can be achieved with different combinations of Cr^{4+} concentrations and thicknesses of Cr^{4+}:YAG ceramic. Higher output pulse energy can be realized with thick saturable absorber and high Cr^{4+} concentration if enough pump power is provided.

The output pulse energy of Yb:YAG/Cr^{4+}:YAG composite ceramics passively Q-switched lasers is not only governed by reflectivity of output coupler and initial transmission of the Cr^{4+}:YAG ceramic, but also is proportional to laser beam area, according to (14). Therefore, the pulse energy can be further scaled by increasing the pump beam diameter when the initial transmission of saturable absorber and reflectivity of the output coupler are fixed. Laser beam

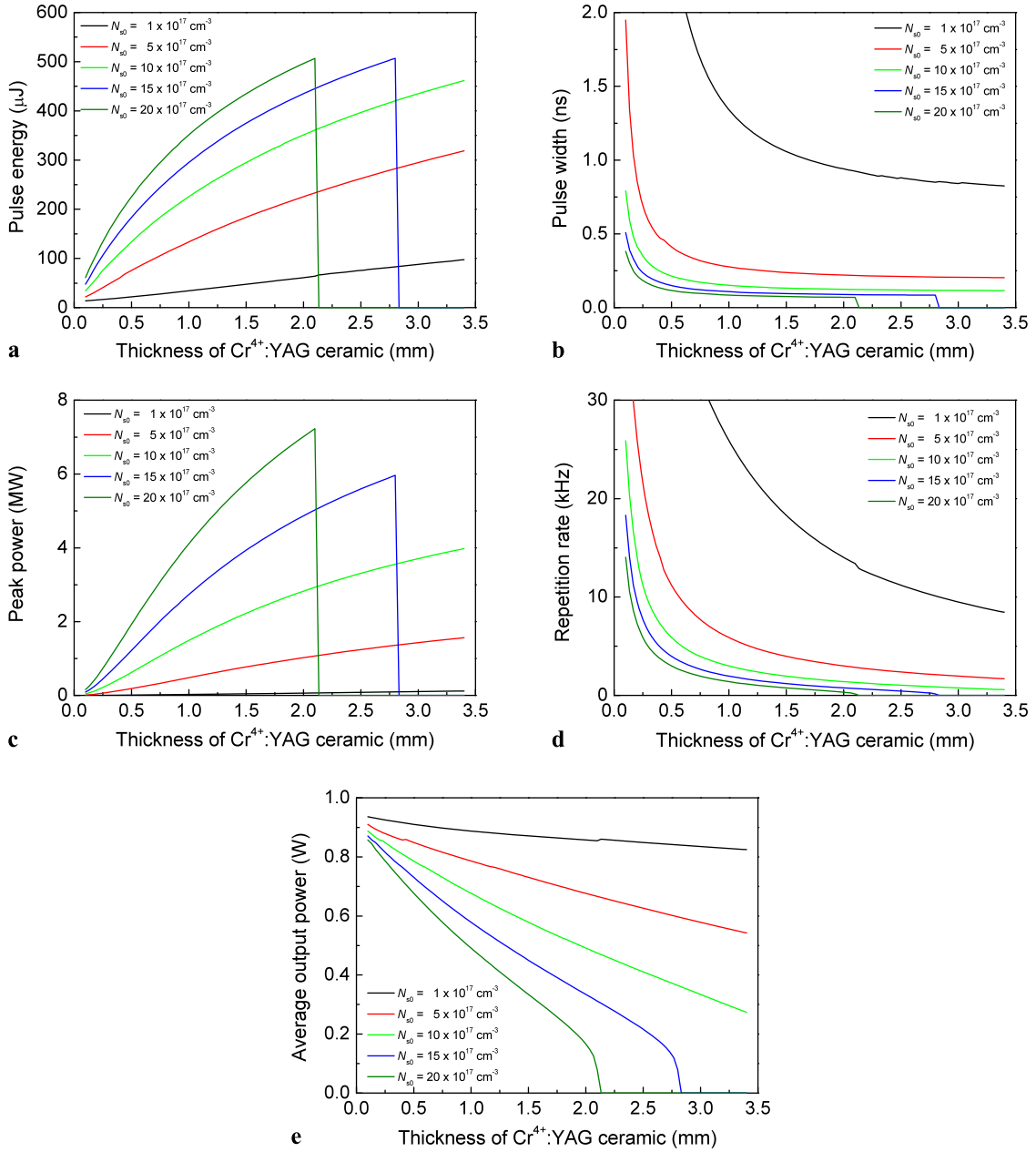

Fig. 4 (**a**) Pulse energy, (**b**) pulse width, (**c**) peak power, (**d**) repetition rate and (**e**) average output power as a function of the thickness of Cr^{4+}:YAG ceramic under incident pump power of 4.5 W

diameter is relative to the pump beam diameter. Yb:YAG is a quasi-three-level system, it requires high pump power intensity to achieve efficient laser oscillation at room temperature [39]. For efficient laser oscillation, the pump power intensity should be high enough to overcome the threshold of passively Q-switched laser, therefore, the high pump power intensity is required for quasi-three-level Yb:YAG/Cr^{4+}:YAG composite ceramics passively Q-switched laser. To achieve high output pulse energy, pump beam diameter should be increased under the condition of certain pump power intensity. Figure 5 shows the pulse energy, pulse width, peak power, repetition rate and average output power as a function of pump beam waist for different Cr^{4+} concentrations. The pump power intensity is 33 kW/cm^2. The thicknesses of Yb:YAG part and Cr^{4+}:YAG part in Yb:YAG/Cr^{4+}:YAG composite ceramics are 1.2 mm and 1.5 mm. Yb doping concentration is 10 at.%. The reflectivity of the output coupler is 50% based on the laser performance obtained in Fig. 3(b).

Figure 5(a) shows the pulse energy increases with pump beam waist for different Cr^{4+} concentrations, the higher the Cr^{4+} concentration, the higher the pulse energy achievable. Pulse energy increases slowly with Cr^{4+} concentra-

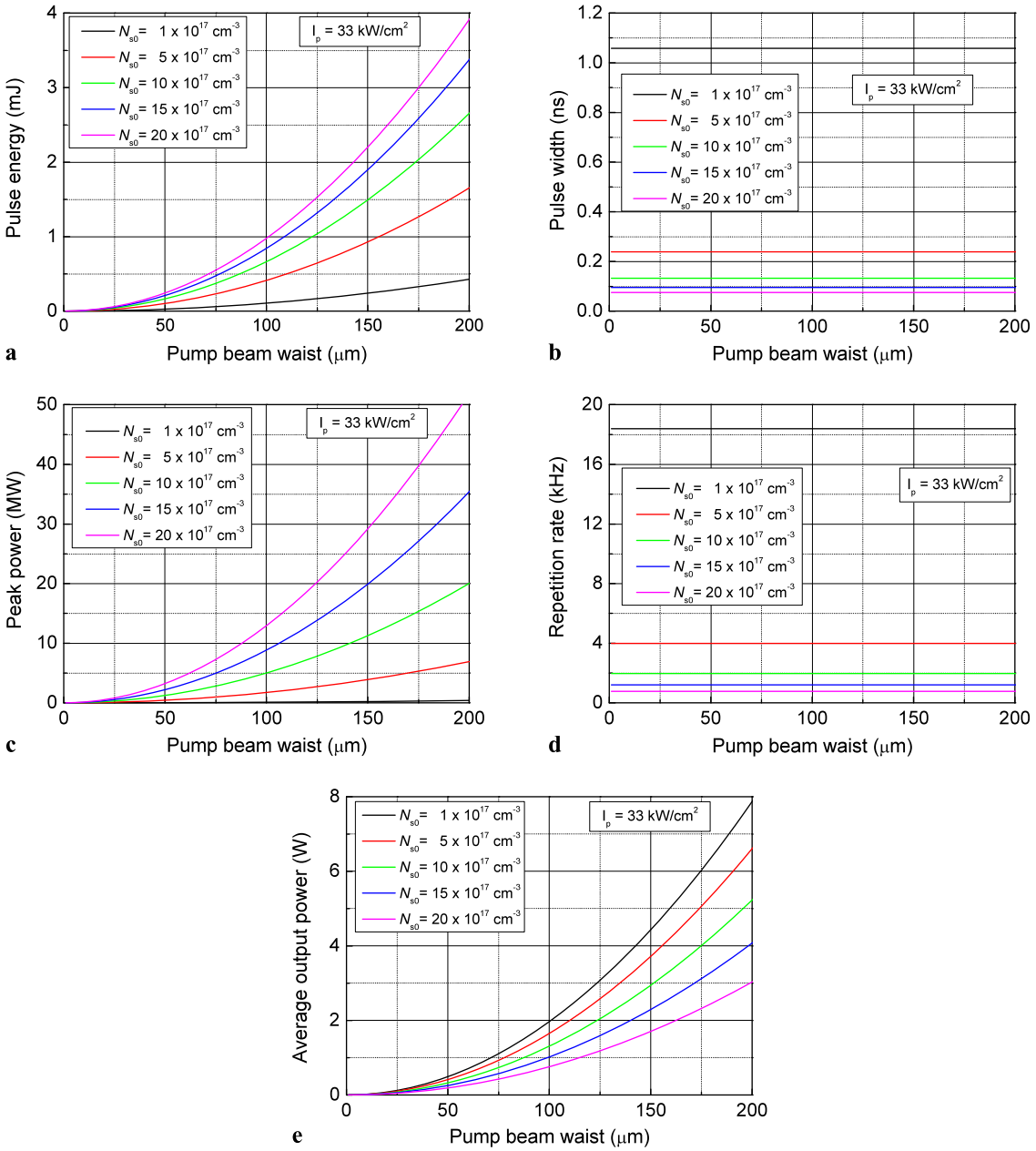

Fig. 5 (**a**) Pulse energy, (**b**) pulse width, (**c**) peak power, (**d**) repetition rate, and (**e**) average output power as a function of pump beam waist for different Cr^{4+} concentration. The pump intensity is 33 kW/cm^2 and the thickness of Yb:YAG and Cr^{4+}:YAG parts in Yb:YAG/Cr^{4+}:YAG composite ceramics are 1.2 mm and 1.5 mm, respectively; reflectivity of the output coupler is 50%

tion at high Cr^{4+} concentration levels for the same pump beam waist. For the constant pump power intensity, the pulse width does not change with pump beam waist for different Cr^{4+} concentrations, the higher the Cr^{4+} concentration, the shorter the pulse width, as shown in Fig. 5(b). The pulse width decreases with Cr^{4+} concentration, and is not sensitive to Cr^{4+} concentration when N_{s0} is greater than 5×10^{17} cm^{-3}. The peak power increases with pump beam waist for different Cr^{4+} concentrations, the higher the Cr^{4+} concentrations, the higher the peak power, as shown in Fig. 5(c). Owing to the constant pump power intensity used in the simulations, the repetition rate dose not change with the pump beam waist for different Cr^{4+} concentrations, the higher the Cr^{4+} concentration, the lower the repetition rate, as shown in Fig. 5(d). Average output power increases with pump beam waist for different Cr^{4+} concentrations, the higher the Cr^{4+} concentration, the lower the average output power, as shown in Fig. 5(e).

From the relationship of the pulse energy as functions of the reflectivity of the output coupler and the thickness

of the saturable absorber, as shown in Figs. 3(a) and 4(a), the higher pulse energy can be obtained by using lower initial transmission of the saturable absorber and lower reflectivity of the output coupler. However, for a practical design of a compact, monolithic Yb:YAG/Cr^{4+}:YAG composite ceramics passively Q-switched laser, adequate pump power should be absorbed by the gain medium to make the laser more efficient, and the loss of the cavity should be kept as low as possible. From Fig. 5, we can see that Yb:YAG/Cr^{4+}:YAG composite ceramics with 1.2-mm-thick-Yb:YAG and 1.5-mm-thick Cr^{4+}:YAG can generate laser pulses with pulse energy of 0.67 mJ, pulse width of 130 ps, peak power of over 5.1 MW for Cr^{4+}:YAG saturable absorber with $N_{s0} = 10 \times 10^{17}$ cm^{-3}. The laser works at 2 kHz, and the average output power of 1.3 W can be generated with 10.6 W incident pump power and pump beam waist of 100 μm; the optical-to-optical efficiency is about 13% with respect to the incident pump power; optical-to-optical efficiency of over 18% can be achieved with respect to the absorbed pump power. For Cr^{4+}:YAG saturable absorber with $N_{s0} = 5 \times 10^{17}$ cm^{-3}, laser pulse with pulse energy of 0.42 mJ and pulse width of 238 ps, resulting peak power of over 1.7 MW can be achieved. The laser works at 4 kHz, the average output power of 1.68 W can be generated with 10.6 W incident pump power and pump beam waist of 100 μm; the optical-to-optical efficiency is about 16% with respect to the incident pump power; optical-to-optical efficiency of over 23% can be achieved with respect to the absorbed pump power.

From these results, we can see that there is a trade-off between laser efficiency and laser characteristics such as pulse energy, pulse width, peak power for laser-diode pump Yb:YAG/Cr^{4+}:YAG composite ceramics passively Q-switched laser. The same pulse energy can be achieved by using different combination of the Cr^{4+} concentration and thickness of Cr^{4+}:YAG ceramic. The pulse width is not sensitive to the Cr^{4+} concentration when the thickness of Cr^{4+}:YAG ceramic is longer than 0.5 mm, as shown in Fig. 4(b). Therefore, better laser performance (short pulse width and high peak power) and good laser efficiency can be achieved by using thin Cr^{4+}:YAG ceramic with high doping concentration and suitable reflectivity of the output coupler.

6 Conclusions

The laser performance of laser-diode end-pumped Yb:YAG/Cr^{4+}:YAG composite ceramics passively Q-switched laser were investigated by numerically solving the modified coupled rate equations including the pump rate term and the excited-state absorption of the saturable absorber of Yb:YAG/Cr^{4+}:YAG composite ceramics passively Q-switched lasers. The laser characteristics of the passively Q-switched lasers as functions of reflectivity of the output coupler, thickness of Cr^{4+}:YAG and pump beam waist were studied analytically by solving the transcendental equation with the aid of Lambert W-function. For Yb:YAG/Cr^{4+}:YAG composite ceramics, optimization of the laser performance can be done by choosing suitable reflectivity of the output coupler, varying the thickness of Cr^{4+}:YAG ceramic and using proper pump beam waist under certain pump power intensity. There is a trade-off between laser characteristics and laser efficiency. The high pulse energy can be obtained with lower reflectivity of the output coupler and lower initial transmission of the saturable absorber. Better laser performance (high peak power and high efficiency) can be achieved using a thin Cr^{4+}:YAG ceramic with high Cr^{4+} concentration, and the suitable reflectivity of the output coupler. The laser characteristics can be predicted by varying the parameters of Yb:YAG/Cr^{4+}:YAG passively Q-switched microchip lasers, this is important for the development of efficient laser-diode pumped Yb:YAG/Cr^{4+}:YAG composite materials passively Q-switched laser used in various applications such as remote ranging, pollution monitoring, laser ignition for engines, and so on.

Acknowledgements This work was supported by Program for New Century Excellent Talents in University (NCET) under Grant No.: NCET-09-0669, the Scientific Research Foundation for the Returned Overseas Chinese Scholars, State Education Ministry (SRF for ROCS, SEM), a grant from the Ph.D. Programs Foundation of Ministry of Education of China (No. 20100121120019), and the Fundamental Research Funds for the Central Universities (grant No. 2010121058). One of us (A.A.K.) is grateful for partial support from the Russian Foundation for Basic Research and the Program of the Presidium of Russian Academy of Sciences "Extreme laser field and their applications".

References

1. G.J. Spuhler, R. Paschotta, M.P. Kullberg, M. Graf, M. Moser, E. Mix, G. Huber, C. Harder, U. Keller, Appl. Phys. B, Lasers Opt. **72**, 285 (2001)
2. J. Dong, P. Deng, Y. Liu, Y. Zhang, J. Xu, W. Chen, X. Xie, Appl. Opt. **40**, 4303 (2001)
3. Y. Kalisky, C. Labbe, K. Waichman, L. Kravchik, U. Rachum, P. Deng, J. Xu, J. Dong, W. Chen, Opt. Mater. **19**, 403 (2002)
4. O.A. Buryy, S.B. Ubiszkii, S.S. Melnyk, A.O. Matkovshii, Appl. Phys. B **78**, 291 (2004)
5. D.S. Sumida, T.Y. Fan, Opt. Lett. **19**, 1343 (1994)
6. T.Y. Fan, IEEE J. Quantum Electron. **29**, 1457 (1993)
7. H.W. Bruesselbach, D.S. Sumida, R.A. Reeder, R.W. Byren, IEEE J. Sel. Top. Quantum Electron. **3**, 105 (1997)
8. J. Dong, M. Bass, Y. Mao, P. Deng, F. Gan, J. Opt. Soc. Am. B **20**, 1975 (2003)
9. F.D. Patel, E.C. Honea, J. Speth, S.A. Payne, R. Hutcheson, R. Equall, IEEE J. Quantum Electron. **37**, 135 (2001)
10. J. Dong, P. Deng, J. Xu, J. Cryst. Growth **203**, 163 (1999)
11. J. Dong, P. Deng, Y. Lu, Y. Zhang, Y. Liu, J. Xu, W. Chen, Opt. Lett. **25**, 1101 (2000)
12. J. Dong, A. Shirakawa, S. Huang, Y. Feng, T. Takaichi, M. Musha, K. Ueda, A.A. Kaminskii, Laser Phys. Lett. **2**, 387 (2005)

13. J. Dong, P. Deng, J. Lumin. **104**, 151 (2003)
14. H. Eilers, U. Hommerich, S.M. Jacobsen, W.M. Yen, K.R. Hoffman, W. Jia, Phys. Rev. B **49**, 15505 (1994)
15. R. Feldman, Y. Shimony, Z. Burshtein, Opt. Mater. **24**, 333 (2003)
16. J.J. Zayhowski, C. Dill III, Opt. Lett. **19**, 1427 (1994)
17. J. Dong, A. Shirakawa, K. Ueda, Appl. Phys. B, Lasers Opt. **85**, 513 (2006)
18. G.J. Spuhler, R. Paschotta, R. Fluck, B. Braun, M. Moser, G. Zhang, E. Gini, U. Keller, J. Opt. Soc. Am. B **16**, 376 (1999)
19. J. Lu, T. Murai, K. Takaichi, T. Uematsu, K. Misawa, M. Prabhu, J. Xu, K. Ueda, H. Yagi, T. Yanagitani, A.A. Kaminskii, A. Kudryashov, Appl. Phys. Lett. **78**, 3586 (2001)
20. J. Lu, K. Takaichi, T. Uematsu, A. Shirakawa, M. Musha, K. Ueda, H. Yagi, T. Yanagitani, A.A. Kaminskii, Jpn. J. Appl. Phys. **41**, L1373 (2002)
21. J. Dong, A. Shirakawa, K. Ueda, H. Yagi, T. Yanagitani, A.A. Kaminskii, Appl. Phys. Lett. **89**, 091114 (2006)
22. S. Nakamura, H. Yoshioka, Y. Matsubara, T. Ogawa, S. Wada, Opt. Commun. **281**, 4411 (2008)
23. J. Dong, A. Shirakawa, K. Takaichi, K. Ueda, H. Yagi, T. Yanagitani, A.A. Kaminskii, Electron. Lett. **42**, 1154 (2006)
24. J. Dong, A. Shirakawa, K. Ueda, H. Yagi, T. Yanagitani, A.A. Kaminskii, Appl. Phys. Lett. **90**, 131105 (2007)
25. T. Yanagitani, H. Yagi, Y. Hiro, Japan Patent 10-101411 (1998)
26. J. Dong, A. Shirakawa, K. Ueda, H. Yagi, T. Yanagitani, A.A. Kaminskii, Appl. Phys. Lett. **90**, 191106 (2007)
27. J. Dong, K. Ueda, A. Shirakawa, H. Yagi, T. Yanagitani, A.A. Kaminskii, Opt. Express **15**, 14516 (2007)
28. J.J. Zayhowski, P.L. Kelley, IEEE J. Quantum Electron. **27**, 2220 (1991)
29. J.J. Degnan, IEEE J. Quantum Electron. **31**, 1890 (1995)
30. G.H. Xiao, M. Bass, IEEE J. Quantum Electron. **33**, 41 (1997)
31. J.J. Degnan, IEEE J. Quantum Electron. **25**, 214 (1989)
32. X. Zhang, S. Zhao, Q. Wang, Q. Zhang, L. Sun, S. Zhang, IEEE J. Quantum Electron. **33**, 2286 (1997)
33. J. Dong, Opt. Commun. **226**, 337 (2003)
34. J. Dong, A. Shirakawa, K. Ueda, Opt. Rev. **12**, 170 (2005)
35. A.E. Siegmann, *Lasers* (University Science, Mill Valley, 1986)
36. J. Dong, Opt. Commun. **226**, 337 (2003)
37. A. Hofer, T. Graf, W. Luthy, H.P. Weber, Laser Phys. Lett. **1**, 282 (2004)
38. R.M. Corless, G.H. Gonnet, D.E.G. Hare, Adv. Comput. Math. **5**, 329 (1996)
39. J. Dong, K. Ueda, Laser Phys. Lett. **2**, 429 (2005)
40. J. Dong, K. Ueda, H. Yagi, A.A. Kaminskii, Z. Cai, Laser Phys. Lett. **6**, 282 (2009)
41. B. Lipavsky, Y. Kalisky, Z. Burshtein, Y. Shimony, S. Rotman, Opt. Mater. **13**, 117 (1999)
42. G. Xiao, J.H. Lim, S. Yang, E.V. Stryland, M. Bass, L. Weichman, IEEE J. Quantum Electron. **35**, 1086 (1999)
43. Z. Burshtein, P. Blau, Y. Kalisky, Y. Shimony, M.R. Kokta, IEEE J. Quantum Electron. **34**, 292 (1998)